

# Scaling Properties of Superfluid $^3\text{He}$ in Aerogel

Gavin Lawes, Simon C.J. Kingsley, Andrei Golov\*,  
Norbert Mulders†, James V. Porto, and Jeevak M. Parpia

*Laboratory of Atomic and Solid State Physics  
Cornell University, Ithaca, New York, 14853*

*†Department of Physics and Astronomy  
University of Delaware, Newark, Delaware*

*We have investigated the superfluid transition of  $^3\text{He}$  in different samples of silica aerogel. Several of these samples have been characterized using x-ray imaging, yielding information about the microstructure of the aerogel. In comparing new measurements on a 99.5% sample with previous observations on the behavior of  $^3\text{He}$  in 98% porous aerogel we have found evidence for a scaling of the superfluid transition temperature to the correlation length of the aerogel. Furthermore, the superfluid density exhibits a similar universal behaviour over a range of values of reduced temperature. We discuss these new results in the context of superfluid pairing in the presence of a correlated disorder, specifically focussing on the fractal nature of the aerogel.*

*PACS numbers: 67.57.Pq*

## 1. INTRODUCTION

The investigation of the superfluid transition of  $^3\text{He}$  in porous silica aerogels has led to a greater understanding of non-conventional Cooper pairing in the presence of disorder. The aerogel provides structural disorder to the  $^3\text{He}$  quasiparticles, and suppresses both  $T_c$  (the superfluid transition temperature) and  $\rho_s$  (the superfluid density)<sup>1,2</sup>. Moreover, this suppression has been shown to be very sensitive to the microstructure of the aerogel— $^3\text{He}$  confined to aerogels with identical porosities but different density correlations exhibits different behaviour<sup>3</sup>. By comparing measurements on aerogel samples with different porosities and microstructure, we have found evidence that the transition temperature and superfluid density of  $^3\text{He}$  in aerogel can be scaled to collapse on universal curves<sup>4</sup>.

### 1.1. Bulk $^3\text{He}$

Bulk  $^3\text{He}$  at low temperatures is a very pure system, free of all impurities. This allows a very precise comparison between experimental results and theoretical predictions, with the result that the properties of bulk  $^3\text{He}$  are well understood. At low temperatures (below  $\approx 2$  mK) the  $^3\text{He}$  quasi-particles condense into  $L=1$   $S=1$  Cooper pairs. The order parameter for superfluid  $^3\text{He}$  is then a complex  $3 \times 3$  tensor ( $A_{\mu i}$ ) with indices for both spin and angular momentum. The size of these Cooper pairs is determined by the coherence length ( $\xi_0$ ), which is a strong function of pressure, varying from  $\approx 150$  Å at high pressure to  $\approx 800$  Å at saturated vapour pressure.

### 1.2. Aerogel Structure

Aerogel is produced by the gelation of  $\text{SiO}_2$  from solution, after which the solvent is removed<sup>5</sup>. This leaves a self-supporting network of silica strands, typically with a very high porosity. The samples studied in these experiments range in porosity from 98% to 99.5%. The density correlations in aerogel exhibit fractal behaviour—the silica network is self-similar on length scales ranging from  $\approx 30$  Å to the aerogel correlation length ( $\xi_a$ ) which is typically greater than  $1,000$  Å. The correlation length  $\xi_a$  is the length scale above which the aerogel appears homogeneous. We have characterized the aerogels in this study by their porosity, fractal dimension ( $D_f$ ) and correlation length ( $\xi_a$ ). The fractal dimension and correlation length are determined by the gelation procedure used in producing the aerogel and may be probed using Small Angle X-Ray Scattering (SAXS).

We used four different aerogel samples for these measurements with different porosities and fractal structures. Samples A and C were investigated using SAXS at the Cornell synchrotron; the values for samples B and D are estimated based on measurements on samples grown under similar conditions<sup>3,6</sup>.

	Porosity	$D_f$	$\xi_a$
Sample A	0.98	1.9	$1300$ Å
Sample B	0.98	1.8	$\approx 900$ Å
Sample C	0.98	1.8	$840$ Å
Sample D	0.995	1.7	$\geq 2000$ Å

Table 1. Parameters that characterize aerogel samples.

Silica aerogel is an ideal substance to use in investigating the effect of

quenched disorder on the superfluid transition of  $^3\text{He}$ . The structural impurity will not be frozen out at low temperatures, the silica is sufficiently dilute to allow the superfluid transition to occur and the length scales present in the aerogel are commensurate with the coherence length of the  $^3\text{He}$ . Previous measurements on the superfluid transition of  $^3\text{He}$  in aerogel using torsional oscillators<sup>1,7</sup>, NMR<sup>2,8</sup> and sound propagation<sup>9</sup> techniques have shown that  $T_c$  and  $\rho_s$  are suppressed in aerogel, but that the superfluid transition remains sharp. This suppression has been shown to depend on not only the porosity of the aerogel sample, but also on the microstructure<sup>3</sup>.

## 2. EXPERIMENTAL DETAILS AND RESULTS

These measurements were done using torsional oscillators operating in self resonant mode. The normal fluid component is viscously coupled to the oscillator. Monitoring the period shift of the oscillator at the superfluid transition allows a precise determination of both  $T_c$  and  $\rho_s$ . The temperature of the cell was measured using a LCMN susceptibility thermometer used in conjunction with a melting curve thermometer. Some of the cells have a small volume of bulk  $^3\text{He}$  in the torsion head. We subtracted off the contribution to the period shift resulting from this bulk  $^3\text{He}$  in determining the superfluid density of the  $^3\text{He}$  in aerogel. The original cells frequently showed sound resonances of the superfluid  $^3\text{He}$ -aerogel system below  $T_c$ . This made it more difficult to determine  $T_c$  and  $\rho_s$ . These resonances were eliminated in the later cell by growing the aerogel in a silver sinter.

### 2.1. Scaling of $T_c$

The superfluid transition temperature of  $^3\text{He}$  in aerogel is suppressed relative to the bulk transition temperature for all aerogel samples. This suppression is shown in Figure 1. The degree of suppression is larger for the higher density aerogels, and all of the samples show the greatest suppression at low pressures (longer coherence lengths).

It is clear that the suppression of  $T_c$  depends on both the porosity of the aerogel and the microstructure of the sample; the  $^3\text{He}$  in the different 98% aerogel samples have different values of  $T_c$ . Figure 2 shows  $T_c$  scaled by the bulk transition temperature plotted against  $\xi_0$  scaled by  $\xi_a$ . This plot suggests that  $T_c$  is determined by the correlation length of the aerogel and not simply by the porosity of the sample. The data for *both* the 99.5% sample and the 98% samples fall on the same universal curve.

We can develop an intuitive idea of why  $T_c$  might depend on the ratio

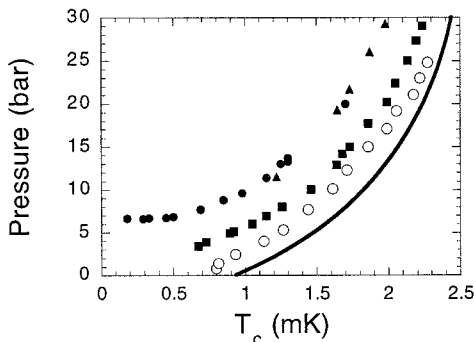


Fig. 1. Pressure versus  $T_c$  for different aerogel samples. Filled squares are cell A, filled triangles are cell B, filled circles are cell C, and empty circles are cell D. The solid line is the superfluid transition curve for bulk  $^3\text{He}$ .

$\xi_0/\xi_a$ . At each position the aerogel strands have some defined direction, so the aerogel should be represented by a vector. Then, in an effective Ginzburg-Landau functional, the lowest order contribution to the free energy consistent with all the symmetry constraints is:

$$f_{\text{aerogel}} = +\delta A_{\mu i}^* A_{\mu j} X_i X_j \quad (1)$$

where  $\delta$  is a coupling parameter,  $X_i$  is some arbitrary potential resulting from the aerogel, and  $A_{\mu i}$  is the superfluid  $^3\text{He}$  order parameter.

We assume that  $X_i$  depends on the density of aerogel at each point. At length scales smaller than  $\xi_0$  the fluctuations in aerogel density are smoothed out because of the coherence of the order parameter. As the temperature dependent coherence length  $\xi(T)$  increases the aerogel density should be averaged over successively larger volumes. At length scales  $b\xi_0$  less than  $\xi_a$  the aerogel density varies like  $b^{d_f-3}$ , where  $d_f$  is the fractal exponent for the aerogel; at longer length scales ( $b\xi_0 > \xi_a$ ) the density is constant. Close to  $T_c$ , when  $\xi(T)$  is very large, the density (and thus  $X_i$ ) is a function of  $(\xi_a/\xi_0)^{d_f-3}$ . Since  $T_c$  is determined by the coefficient of the quadratic term in the full free energy functional, the suppression of  $T_c$  should also be a function of  $(\xi_a/\xi_0)^{d_f-3}$ .

The simplest form of this function would have  $|X_i| \propto \text{density}$ , which results in  $T_c/T_{c0} = 1 - \delta(\xi_a/\xi_0)^{2d_f-6}$ . This function is plotted for  $d_f=1.85$  in Figure 2, where  $\delta$  is fixed by the requirement that  $T_c/T_{c0}=0$  when  $\xi_0/\xi_a = 0.48$ .

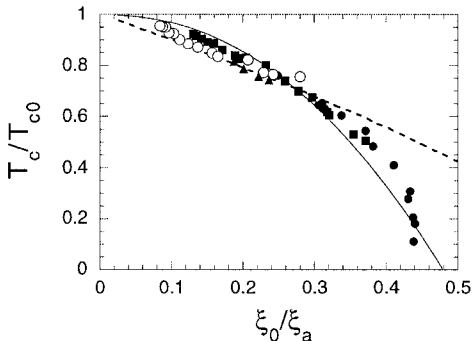


Fig. 2. Suppression of  $T_c$  versus  $\xi_0/\xi_a$ . The symbols are the same used in Figure 1. The dashed line is derived from the HSM<sup>11</sup> and the solid line results from the argument described above.

## 2.2. Scaling of $\rho_s$

The superfluid density of  $^3\text{He}$  is also suppressed in aerogel relative to bulk. Experimentally, we find that this suppression is much larger than would be predicted using an Abrikosov-Gorkov model<sup>10</sup> and is very strongly dependent on pressure. Motivated by the Abrikosov-Gorkov equation, we plot the superfluid density (more precisely the bare superfluid density  $\rho_s^b/\rho = ((1 + \frac{1}{3}F_1)\frac{\rho_s}{\rho})/(1 + \frac{1}{3}F_1\frac{\rho_s}{\rho}))$  of  $^3\text{He}$  in aerogel, scaled by the bulk density, versus the square of  $T_c$  scaled by the bulk transition temperature, for several different values of reduced temperature. This is presented in Figure 3.

The data for  $T=0.6T_c$ ,  $T=0.7T_c$  and  $T=0.8T_c$ , for all the aerogel samples, collapse on a universal curve which has a characteristic shape different from the homogeneous scattering model (HSM) of Thuneberg *et al.*<sup>11</sup>. The steep slope of the curve suggests an absence of a characteristic length scale in the disorder<sup>12</sup> and emphasizes the importance of the fractal distribution of the aerogel. The collapse for different reduced temperatures may also result from fractal correlations in the disorder. Since all of the aerogel samples studied have approximately the same fractal dimension, this universal curve must be fixed by  $\xi_a$ .

## 3. CONCLUSIONS AND ACKNOWLEDGMENTS

The suppression of  $T_c$  and  $\rho_s$  of  $^3\text{He}$  in aerogel varies with the porosity and microstructure of the sample. We have shown that, when scaled by their bulk values, both  $T_c$  and  $\rho_s$  collapse onto universal curves for all the aerogel

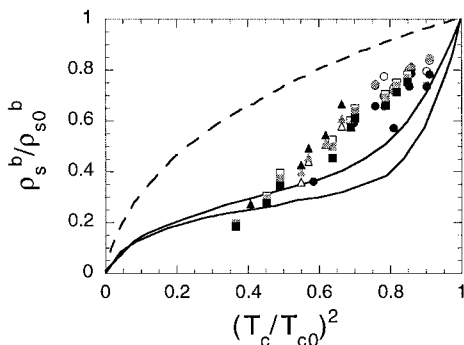


Fig. 3. Bare superfluid density at  $T=0.6T_c$  (open symbols),  $T=0.7T_c$  (gray symbols), and  $T=0.8T_c$  (black symbols). Cell A is the squares, cell B the triangles and cell D the circles. The dashed line is predicted by the HSM<sup>11</sup>, while the solid lines are computed from the isotropic inhomogeneous scattering model (IISM) for  $T=0.7T_c$  (top) and  $T=0.8T_c$  (bottom)<sup>12</sup>.

samples investigated. This scaling may be traced to the fractal nature of the disorder. Models which incorporate length scales in the description of the disorder have not predicted this universal behaviour. The  $^3\text{He}$ -aerogel system is thus well suited to the investigation of correlated disorder on critical behaviour.

We acknowledge helpful conversations with T.L. Ho, J. Beamish, M.H.W. Chan, D. Ponarin and E. Thuneberg. This research was supported by the NSF under DMR-9705295 and DMR-9970817.

## REFERENCES

[\*] Now at Dept. of Physics and Astronomy, Univ. of Manchester, UK.

1. J.V. Porto and J.M. Parpia, *Phys. Rev. Lett.* **74**, 4667 (1995).
2. D.T. Sprague *et al.*, *Phys. Rev. Lett.* **75**, 661 (1995).
3. J.V. Porto and J.M. Parpia, *Phys. Rev. B* **59**, 14584 (1999).
4. G. Lawes *et al.*, *Phys. Rev. Lett.* **84**, 4148 (2000).
5. D. W. Schaefer and K. D. Keefer, *Phys. Rev. Lett.* **56**, 2199 (1986).
6. L. Lurio *et al.*, [http://bnlinfo2.bnl.gov:80/nsls97/toc/toc\\_X20C.html](http://bnlinfo2.bnl.gov:80/nsls97/toc/toc_X20C.html).
7. K. Matsumoto *et al.*, *Phys. Rev. Lett.* **79**, 273 (1997).
8. H. Alles *et al.*, *Physica B* **255**, 1 (1998).
9. A. Golov *et al.*, *Phys. Rev. Lett.* **82**, 3492 (1999).
10. A. A. Abrikosov and L. P. Gorkov, *Sov. Phys. JETP* **12**, 1243 (1961).
11. E. V. Thuneberg *et al.*, *Phys. Rev. Lett.* **80**, 2861 (1998).
12. E.V. Thuneberg, private communication.